

Syntheses, structures, and properties of $\text{Ag}_4(\text{Mo}_2\text{O}_5)(\text{SeO}_4)_2(\text{SeO}_3)$ and $\text{Ag}_2(\text{MoO}_3)_3\text{SeO}_3$

Jie Ling, Thomas E. Albrecht-Schmitt*

Department of Chemistry and Biochemistry, 179 Chemistry Building, Auburn University, Auburn, AL 36849, USA

Received 30 January 2007; received in revised form 21 February 2007; accepted 23 February 2007

Available online 7 March 2007

Abstract

$\text{Ag}_4(\text{Mo}_2\text{O}_5)(\text{SeO}_4)_2(\text{SeO}_3)$ has been synthesized by reacting AgNO_3 , MoO_3 , and selenic acid under mild hydrothermal conditions. The structure of this compound consists of *cis*- MoO_2^{2+} molybdenyl units that are bridged to neighboring molybdenyl moieties by selenate anions and by a bridging oxo anion. These dimeric units are joined by selenite anions to yield zigzag one-dimensional chains that extended down the *c*-axis. Individual chains are polar with the C_2 distortion of the Mo(VI) octahedra aligning on one side of each chain. However, the overall structure is centrosymmetric because neighboring chains have opposite alignment of the C_2 distortion. Upon heating $\text{Ag}_4(\text{Mo}_2\text{O}_5)(\text{SeO}_4)_2(\text{SeO}_3)$ loses SeO_2 in two distinct steps to yield Ag_2MoO_4 . Crystallographic data: (193 K; $\text{MoK}\alpha$, $\lambda = 0.71073 \text{ \AA}$): orthorhombic, space group *Pbcm*, $a = 5.6557(3)$, $b = 15.8904(7)$, $c = 15.7938(7) \text{ \AA}$, $V = 1419.41(12)$, $Z = 4$, $R(F) = 2.72\%$ for 121 parameters with 1829 reflections with $I > 2\sigma(I)$. $\text{Ag}_2(\text{MoO}_3)_3\text{SeO}_3$ was synthesized by reacting AgNO_3 with MoO_3 , SeO_2 , and HF under hydrothermal conditions. The structure of $\text{Ag}_2(\text{MoO}_3)_3\text{SeO}_3$ consists of three crystallographically unique Mo(VI) centers that are in $2 + 2 + 2$ coordination environments with two long, two intermediate, and two short bonds. These MoO_6 units are connected to form a molybdenyl ribbon that extends along the *c*-axis. These ribbons are further connected together through tridentate selenite anions to form two-dimensional layers in the *[bc]* plane. Crystallographic data: (193 K; $\text{MoK}\alpha$, $\lambda = 0.71073 \text{ \AA}$): monoclinic, space group $P2_1/n$, $a = 7.7034(5)$, $b = 11.1485(8)$, $c = 12.7500(9) \text{ \AA}$, $\beta = 105.018(1)$, $V = 1002.7(2)$, $Z = 4$, $R(F) = 3.45\%$ for 164 parameters with 2454 reflections with $I > 2\sigma(I)$. $\text{Ag}_2(\text{MoO}_3)_3\text{SeO}_3$ decomposes to $\text{Ag}_2\text{Mo}_3\text{O}_{10}$ on heating above 550°C .
© 2007 Elsevier Inc. All rights reserved.

Keywords: Transition metal selenate selenite; Transition metal selenite; Thermal behavior; Hydrothermal synthesis

1. Introduction

Mixed-valent selenate selenite compounds that contain Se(VI) in form of SeO_4^{2-} and Se(IV) in SeO_3^{2-} represent a growing family of transition metal and f-block oxoanion solids that display new structural motifs and important optical properties. This family includes a single mineral, schmiederit, $\text{Pb}_2\text{Cu}_2(\text{OH})_4(\text{SeO}_3)(\text{SeO}_4)$ [1], five lanthanide compounds, $\text{Er}_2(\text{SeO}_3)_2(\text{SeO}_4) \cdot 2\text{H}_2\text{O}$ [2], $\text{La}(\text{HSeO}_3)(\text{SeO}_4) \cdot 2\text{H}_2\text{O}$ [3], $\text{Nd}_2(\text{SeO}_4)(\text{SeO}_3)_2(\text{H}_2\text{O})_2$ [4], $\text{Pr}_4(\text{SeO}_3)_2(\text{SeO}_4)_6$ [5], $\text{NaSm}(\text{SeO}_3)(\text{SeO}_4)$ [5], the hydrated double salt, $\text{Na}_2\text{SeO}_4 \cdot \text{H}_2\text{SeO}_3 \cdot \text{H}_2\text{O}$ [6], the five transition metal compounds $\text{Li}_2\text{Cu}_3(\text{SeO}_3)_2(\text{SeO}_4)_2$ [7], $\text{Hg}_3(\text{SeO}_3)_2(\text{SeO}_4)$ [8], $\text{Fe}(\text{HSeO}_3)(\text{SeO}_4) \cdot \text{H}_2\text{O}$ [9], $\text{RbFe}(\text{SeO}_3)(\text{SeO}_4)$ [9], and

$\text{Au}_2(\text{SeO}_3)_2(\text{SeO}_4)$ [10], and three early actinide-containing solids, $\text{Th}(\text{SeO}_3)(\text{SeO}_4)$ [11], $[\text{C}_5\text{H}_{14}\text{N}][\text{UO}_2(\text{SeO}_4)(\text{SeO}_2\text{OH})]$ [12], and $[\text{C}_5\text{H}_{14}\text{N}]_4[(\text{UO}_2)_3(\text{SeO}_4)_4(\text{HSeO}_3)(\text{H}_2\text{O})(\text{H}_2\text{SeO}_3)(\text{HSeO}_4)]$ [13].

One of the reasons for investigating this group of compounds is to investigate the effect that the lone-pair of electrons on the selenite anions has on the local and extended structures. In this regard there are several known effects. First, small channels and cavities often form to house the lone-pair of electrons as occurs in $\beta\text{-AgNpO}_2(\text{SeO}_3)$ [14]. Second, lone-pair alignment selenite can take place to yield polar structures (e.g. in $\text{Au}_2(\text{SeO}_3)_2(\text{SeO}_4)$ [10] and $A_2(\text{MoO}_3)_3\text{SeO}_3$ ($A = \text{Rb}, \text{Cs}, \text{Tl}, \text{NH}_4$) [15]. When the latter effect occurs the materials are capable of displaying a wide variety of important properties including nonlinear optical behavior, as well as pyro-, piezo-, and ferroelectricity [16,17]. In this report we disclose the

*Corresponding author. Fax: +1 334 844 6959.

E-mail address: albreth@auburn.edu (T.E. Albrecht-Schmitt).

synthesis, structure, vibrational spectroscopy, and thermal behavior of the new Mo(VI) selenate selenite, $\text{Ag}_4(\text{Mo}_2\text{O}_5)(\text{SeO}_4)_2(\text{SeO}_3)$. This compound contains polar chains, however, the overall structure is centrosymmetric. In addition, we also provide information on a new member of the $A_2(\text{MoO}_3)_3\text{SeO}_3$ ($A = \text{Rb}, \text{Cs}, \text{Tl}, \text{NH}_4$) family [15], $\text{Ag}_2(\text{MoO}_3)_3\text{SeO}_3$, whose structure differs significantly from previous members.

2. Experimental

AgNO_3 (99.9%, Alfa-Aesar), MoO_3 (99.95%, Alfa-Aesar), H_2SeO_4 (40%, Alfa-Aesar), SeO_2 (99.4%, Alfa-Aesar) and HF (48%, Alfa-Aesar) were used as received without further purification. Distilled and Millipore filtered water with resistance of 18.2 M Ω cm was used in all reactions. SEM/EDX analyses were performed using a JEOL JSM-7000F. Silver, molybdenum, and selenium standards were used to calibrate the results.

$\text{Ag}_4(\text{Mo}_2\text{O}_5)(\text{SeO}_4)_2(\text{SeO}_3)$ was synthesized by loading AgNO_3 (185.4 mg, 1.091 mmol), MoO_3 (235.6 mg, 1.637 mmol), H_2SeO_4 (1.00 mL, 3.89 mmol), and 0.5 mL water in a 23-mL PTFE-lined autoclave. The autoclave was sealed and heated at 200 °C in a box furnace. After 3 days, the furnace was cooled to room temperature at a rate of 9 °C/h. The reaction product contained a single phase of pale yellow crystals immersed in a colorless mother liquor. The product was washed with water and methanol and allowed to dry. Yield: 271 mg (88.8% based on Ag). EDX analysis provided Ag:Mo:Se ratio of 4:2:3 (44%:23%:33%).

$\text{Ag}_2(\text{MoO}_3)_3\text{SeO}_3$ was synthesized by loading AgNO_3 (192.5 mg, 1.133 mmol), MoO_3 (244.6 mg, 1.699 mmol), SeO_2 (62.9 mg, 0.567 mmol), HF (0.1 mL, 2.76 mmol), and 0.5 mL water in a 23-mL PTFE-lined autoclave. The autoclave was sealed and heated at 180 °C in a box furnace. After 4 days, the furnace was cooled to room temperature at a rate of 9 °C/h. The product was washed with water and methanol. Orange crystals and an unidentified yellow powder were left to dry in the air. Yield: 272 mg (62.1% based on Ag). EDX analysis of the orange crystals provided a Ag:Mo:Se ratio of 2:3:1 (34%:50%:16%).

2.1. Crystallographic studies

Single crystals of $\text{Ag}_4(\text{Mo}_2\text{O}_5)(\text{SeO}_4)_2(\text{SeO}_3)$ and $\text{Ag}_2(\text{MoO}_3)_3\text{SeO}_3$ with dimensions of 0.106 mm \times 0.072 mm \times 0.035 mm and 0.102 mm \times 0.052 mm \times 0.028 mm, respectively, were selected and mounted on two quartz fibers with epoxy and aligned on a Bruker SMART APEX CCD X-ray diffractometer with a digital camera. Intensity measurements were performed using graphite monochromated Mo $K\alpha$ radiation from a sealed tube with a monocapillary collimator. The intensities and positions of reflections of a sphere were collected by a combination of 3 sets of exposure frames. Each set had a different ϕ angle

for the crystal and each exposure covered a range of 0.3° in ω . A total of 1800 frames were collected with an exposure time per frame of 20 s for $\text{Ag}_4(\text{Mo}_2\text{O}_5)(\text{SeO}_4)_2(\text{SeO}_3)$ and 10 s for $\text{Ag}_2(\text{MoO}_3)_3\text{SeO}_3$.

Determination of integrated intensities and global cell refinement were performed with the Bruker SAINT (v 6.02) software package using a narrow-frame integration algorithm. A semi-empirical absorption correction was applied using SADABS [18]. The program suite SHELXTL (v 5.1) was used for space group determination (XPREP), direct methods structure solution (XS), and least-squares refinement (XL) [19]. The final refinements included anisotropic displacement parameters for all atoms and a secondary extinction parameter. Some crystallographic details are listed in Table 1, and the final positional parameters can be found in Tables 2 and 3. Further details of the crystal structure investigations may be obtained from the Fachinformatiozentrum Karlsruhe, D-76344 Eggenstein-Leopoldshafen, Germany (Fax: (+49)7247-808-666; Email: crysdata@fiz-karlsruhe.de) on quoting the depository numbers CSD 417618 and 417617 for $\text{Ag}_4(\text{Mo}_2\text{O}_5)(\text{SeO}_4)_2(\text{SeO}_3)$ and $\text{Ag}_2(\text{MoO}_3)_3\text{SeO}_3$, respectively.

2.1.1. Vibrational spectroscopy

The IR spectra of $\text{Ag}_4(\text{Mo}_2\text{O}_5)(\text{SeO}_4)_2(\text{SeO}_3)$ and $\text{Ag}_2(\text{MoO}_3)_3\text{SeO}_3$ were taken from samples in KBr pellets with using a Shimadzu IR Prestige-21 in the wave number range of 4000–400 cm^{-1} . Raman spectroscopy experiments were performed at room temperature using backscattering geometry with 514.5 nm (2.41 eV) line of an argon-ion laser and an ISA U-1000 scanning double monochromator to disperse the Stokes Raman scattering spectra.

Table 1
Crystallographic data for $\text{Ag}_4(\text{Mo}_2\text{O}_5)(\text{SeO}_4)_2(\text{SeO}_3)$ and $\text{Ag}_2(\text{MoO}_3)_3\text{SeO}_3$

Formula	$\text{Ag}_4(\text{Mo}_2\text{O}_5)(\text{SeO}_4)_2(\text{SeO}_3)$	$\text{Ag}_2(\text{MoO}_3)_3\text{SeO}_3$
Formula mass	1116.24	774.52
Color and habit	Yellow, block	Orange, block
Crystal system	Orthorhombic	Monoclinic
Space group	<i>Pbcm</i> (No. 57)	<i>P2₁/n</i> (No.14)
<i>a</i> (Å)	5.6557(3)	7.3034(5)
<i>b</i> (Å)	15.8904(7)	11.1485(8)
<i>c</i> (Å)	15.7938(7)	12.7500(9)
α (deg)	90	90
β (deg)	90	105.018(1)
γ (deg)	90	90
<i>V</i> (Å ³)	1419.4(1)	1002.7(2)
<i>Z</i>	4	4
<i>T</i> (K)	193	193
λ (Å)	0.71073	0.71073
Maximum 2θ (°)	56.62	56.58
ρ_{calcd} (g cm ⁻³)	5.223	5.131
μ (Mo $K\alpha$) (cm ⁻¹)	149.05	111.78
<i>R</i> (<i>F</i>) for $F_o^2 > 2\sigma(F_o^2)^a$	0.0272	0.0345
$R_w(F_o^2)^b$	0.0661	0.0833

$$^a R(F) = \frac{\sum ||F_o| - |F_c||}{\sum |F_o|}$$

$$^b R_w(F_o^2) = \left[\frac{\sum [w(F_o^2 - F_c^2)]^2}{\sum wF_o^4} \right]^{1/2}$$

Table 2
Atomic coordinates and equivalent isotopic displacement parameters for $\text{Ag}_4(\text{Mo}_2\text{O}_5)(\text{SeO}_4)_2(\text{SeO}_3)$

Atom(site)	x	y	z	$U_{\text{eq}} (\text{\AA}^2)^a$
Ag(1)	0.17767(10)	0.34503(4)	$\frac{1}{4}$	0.01739(13)
Ag(2)	0.69721(10)	0.50077(3)	$\frac{1}{4}$	0.01628(13)
Ag(3)	0.17562(7)	0.50367(2)	0.42003(3)	0.01659(11)
Mo(1)	0.64349(7)	0.67226(3)	0.41167(2)	0.00993(11)
Se(1)	0.24643(12)	0.63408(4)	$\frac{1}{4}$	0.01036(14)
Se(2)	0.67276(8)	0.35891(3)	0.39988(3)	0.01122(12)
O(1)	0.4373(6)	0.6037(2)	0.3320(2)	0.0154(7)
O(2)	0.0814(10)	0.5493(3)	$\frac{1}{4}$	0.0240(12)
O(3)	0.3496(6)	0.7579(2)	0.3787(2)	0.0166(7)
O(4)	0.6559(6)	0.3745(2)	0.5031(2)	0.0160(7)
O(5)	0.9259(7)	0.3933(2)	0.3647(2)	0.0207(8)
O(6)	0.4597(7)	0.4102(2)	0.3515(2)	0.0201(8)
O(7)	0.1765(7)	0.2146(2)	0.1627(2)	0.0189(8)
O(8)	0.7973(6)	0.5849(2)	0.4450(2)	0.0168(7)
O(9)	0.6977(8)	$\frac{3}{4}$	$\frac{1}{2}$	0.0132(9)

Table 3
Atomic coordinates and equivalent isotopic displacement parameters for $\text{Ag}_2(\text{MoO}_3)_3\text{SeO}_3$

Atom(site)	x	y	z	$U_{\text{eq}} (\text{\AA}^2)^a$
Mo(1)	-0.41376(5)	0.40227(3)	0.80118(3)	0.00636(12)
Mo(2)	-0.44934(5)	0.07632(3)	0.81194(3)	0.00635(12)
Mo(3)	0.15004(6)	0.08270(3)	0.94463(3)	0.00637(12)
Ag(1)	0.13073(6)	0.41724(3)	0.93163(2)	0.01347(12)
Ag(2)	-0.14522(6)	0.24812(3)	0.05667(3)	0.01355(12)
Se(1)	-0.15215(6)	0.19103(4)	0.69478(3)	0.00888(13)
O(1)	0.2569(5)	0.0813(3)	0.8413(3)	0.0149(8)
O(2)	0.3410(5)	0.0749(3)	0.0545(3)	0.0143(8)
O(3)	-0.1195(5)	0.0967(3)	0.8039(3)	0.0113(7)
O(4)	0.0588(5)	-0.0811(3)	0.9479(3)	0.0092(7)
O(5)	0.0857(5)	0.2486(2)	0.9649(3)	0.0087(7)
O(6)	-0.0541(5)	0.4132(3)	0.8162(3)	0.0125(7)
O(7)	0.3099(5)	0.4144(3)	0.0948(3)	0.0120(7)
O(8)	0.3220(5)	0.4167(3)	0.8805(3)	0.0160(8)
O(9)	0.0986(5)	0.5828(3)	0.9663(3)	0.0092(7)
O(10)	-0.3352(5)	0.2368(3)	0.9448(3)	0.0149(8)
O(11)	-0.2494(5)	0.2440(3)	0.1603(3)	0.0156(8)
O(12)	0.1204(5)	0.2661(3)	0.1905(3)	0.0102(7)

2.1.2. Thermal analysis

For the investigation of the thermal behavior, 25 mg of the title compounds were placed in two platinum pans that were heated (5 °C/min) up to 725 °C under a nitrogen flow using a TGA Instruments Model Q50 V5.3 Build 171. The residue compositions were checked by power X-ray diffraction.

2.1.3. Powder X-ray diffraction

Powder X-ray diffraction patterns were collected with a Rigaku Miniflex powder X-ray diffractometer using Cu $K\alpha$ ($\lambda = 1.54056 \text{ \AA}$) radiation. The collected patterns were compared with that calculated from single crystal data using ATOMS [20].

3. Results and discussion

3.1. Synthesis of $\text{Ag}_4(\text{Mo}_2\text{O}_5)(\text{SeO}_4)_2(\text{SeO}_3)$

There are a number of methods that have been applied to the synthesis of mixed-valent selenate selenite compounds. Under hydrothermal conditions, SeO_4^{2-} can be reduced to SeO_3^{2-} as occurs in the preparation of $\text{Au}_2(\text{SeO}_3)_2(\text{SeO}_4)$ [10]. In the synthesis of $\text{Nd}_2(\text{SeO}_4)(\text{SeO}_3)_2(\text{H}_2\text{O})_2$, a portion of the SeO_4^{2-} was reduced to SeO_3^{2-} with 1,10-phenanthroline [4]. $\text{Na}_2\text{SeO}_4 \cdot \text{H}_2\text{SeO}_3 \cdot \text{H}_2\text{O}$ was prepared by slow evaporation of an aqueous solution containing Na_2SeO_4 and H_2SeO_3 at room temperature [6]. Mixed-valent Se(IV)/Se(VI) compounds can also be obtained by oxidizing SeO_2 with HNO_3 , e.g. in the preparation of $\text{Er}_2(\text{SeO}_3)_2(\text{SeO}_4) \cdot 2\text{H}_2\text{O}$ [2].

In this work, $\text{Ag}_4(\text{Mo}_2\text{O}_5)(\text{SeO}_4)_2(\text{SeO}_3)$ was prepared as a pure phase by reacting AgNO_3 , MoO_3 , and H_2SeO_4 under mild hydrothermal conditions. Here some of the SeO_4^{2-} was reduced to SeO_3^{2-} as occurs in the preparation of $\text{Th}(\text{SeO}_3)(\text{SeO}_4)$ [11]. There are two options for explaining the reduction of selenate to selenite. The first of these is that the relatively strong oxidizing power of selenate ($E^\circ = 1.151 \text{ V}$) might be sufficient under these conditions to oxidize water. Second, the selenate might thermally decompose to yield selenite. The moderate heating conditions used here allow for the isolation of partially reduced compounds. The synthesis of $\text{Ag}_4(\text{Mo}_2\text{O}_5)(\text{SeO}_4)_2(\text{SeO}_3)$ is quite reproducible, and occurs in high yield suggesting that an impurity is not responsible for the reduction of the selenate anion.

Orange crystals of $\text{Ag}_2(\text{MoO}_3)_3\text{SeO}_3$ were synthesized hydrothermally by reacting AgNO_3 , MoO_3 , SeO_2 , and HF. Although fluoride is not incorporated in the compound, HF apparently plays an important role in the synthesis because attempts to prepare $\text{Ag}_2(\text{MoO}_3)_3\text{SeO}_3$ in the absence of HF were unsuccessful. The substitution of nitric acid for hydrofluoric acid was not successful. Fluoride is probably serving as a mineralizing agent.

3.2. Crystal structure of $\text{Ag}_4(\text{Mo}_2\text{O}_5)(\text{SeO}_4)_2(\text{SeO}_3)$

The structure of the title compound contains one crystallographically unique Mo(VI) center in classical 2+2+2 coordination environments with two long, two intermediate, and two short bonds. The bond distances Mo(1) are 1.694(4), 1.721(4), 1.889(4), 2.032(4), 2.210(4), and 2.288(4) Å. The two shortest bonds define MoO_2^{2+} molybdenyl units where the oxo atoms are terminal. The Mo centers are shifted along a C_2 -axis of each octahedron by 0.356(1) Å from the center of the six oxygen atoms. The MoO_6 units share a single corner to create dimers. The bridging Mo(1)–O(9) bond has a bond distance of 1.889(1) Å, and a Mo(1)–O(9)–Mo(1) angle of 161.3(3)° that are typical when compared with previously reported crystallographic data of Mo_2O_{11} units [21–23]. Within each

dimer two selenate anions bridge the Mo(VI) centers. The dimers are in turn linked into zigzag one-dimensional chains by selenite anions, as is shown in Fig. 1. The chains extend down the *c*-axis. Individual chains are polar with the C_2 distortion of the Mo(VI) octahedra aligning on one side of each chain. However, the overall structure is centrosymmetric because neighboring chains have opposite alignment of the C_2 distortion, as is depicted in Fig. 2. The bridging selenite anions contain a stereochemically active lone-pair of electrons that oppositely align in the *b* direction, resulting in a cancellation of polarity produced by this group. There are no long contacts between the Se atom in the selenite anion and neighboring oxygen atoms within the structure. Selected bond distances and bond angles are given in Table 4. The calculated bond-valence sum (BVS) of Mo(1) is 5.994 [24,25].

Se(1) is coordinated by three oxygen atoms in a trigonal pyramidal geometry with Se(1)–O bond distances of 1.638(5) Å (terminal) and 1.754(3) Å (bridging). Se(2) is

Table 4

Selected bond distances (Å) and angles (deg) for $\text{Ag}_4(\text{Mo}_2\text{O}_5)(\text{SeO}_4)_2(\text{SeO}_3)$

Bond distances (Å)			
Mo(1)–O(1)	2.032(4)	Se(1)–O(1) x 2	1.754(3)
Mo(1)–O(3)	2.210(4)	Se(1)–O(2)	1.638(5)
Mo(1)–O(4)	2.288(4)	Se(2)–O(3)	1.645(4)
Mo(1)–O(7)	1.694(4)	Se(2)–O(4)	1.651(4)
Mo(1)–O(8)	1.721(4)	Se(2)–O(5)	1.630(4)
Mo(1)–O(9)	1.889(1)	Se(2)–O(6)	1.643(4)
Angles (deg)			
O(1)–Mo(1)–O(3)	75.7(1)	O(7)–Mo(1)–O(9)	98.9(2)
O(1)–Mo(1)–O(4)	76.4(1)	O(8)–Mo(1)–O(9)	102.7(2)
O(1)–Mo(1)–O(7)	97.4(2)	Mo(1)–O(9)–Mo(1)	161.3(3)
O(1)–Mo(1)–O(8)	92.7(2)		
O(1)–Mo(1)–O(9)	154.3(2)	O(1)–Se(1)–O(1)	95.2(2)
O(3)–Mo(1)–O(4)	77.4(1)	O(1)–Se(1)–O(2)	97.2(2)
O(3)–Mo(1)–O(7)	92.6(2)	O(1)–Se(1)–O(2)	97.2(2)
O(3)–Mo(1)–O(8)	161.6(2)	O(3)–Se(2)–O(4)	110.0(2)
O(3)–Mo(1)–O(9)	83.9(1)	O(3)–Se(2)–O(5)	109.0(2)
O(4)–Mo(1)–O(7)	169.2(2)	O(3)–Se(2)–O(6)	109.5(2)
O(4)–Mo(1)–O(8)	86.1(2)	O(4)–Se(2)–O(5)	109.7(2)
O(4)–Mo(1)–O(9)	84.2(1)	O(4)–Se(2)–O(6)	110.0(2)
O(7)–Mo(1)–O(8)	154.3(2)	O(5)–Se(2)–O(6)	108.6(2)

present in a tetrahedral environment, and has Se(2)–O bonds averaging 1.642(4) Å. The calculated bond valence sums of Se(1) and Se(2) are 3.932 and 5.897, respectively [24,25].

There are three crystallographically unique Ag^+ centers in the structure of $\text{Ag}_4(\text{Mo}_2\text{O}_5)(\text{SeO}_4)_2(\text{SeO}_3)$. Ag(1) resides in a trigonal prismatic environment with Ag–O bond distances ranging from 2.429(4) to 2.490(4) Å. Ag(2) and Ag(3) are five- and six-coordinate, respectively, and both have highly irregular geometries. Ag(2) has Ag–O bond distances in the range of 2.306(6)–2.553(4) Å, while those of Ag(3) range from 2.415(4) to 2.579(4) Å. The calculated bond valence sums of Ag(1), Ag(2), and Ag(3) are 1.001, 0.798, and 0.929, respectively [24,25].

3.2.1. Crystal structure of $\text{Ag}_2(\text{MoO}_3)_3\text{SeO}_3$

Although $\text{Ag}_2(\text{MoO}_3)_3\text{SeO}_3$ has a similar formula with $A_2(\text{MoO}_3)_3\text{SeO}_3$ ($A = \text{Rb}, \text{Cs}, \text{Tl}, \text{NH}_4$), it crystallizes in the monoclinic space group $P2_1/n$ instead of the hexagonal space group $P6_3$ [15]. The $A_2(\text{MoO}_3)_3\text{SeO}_3$ ($A = \text{Rb}, \text{Cs}, \text{Tl}, \text{NH}_4$) family of compounds consists of two-dimensional anionic slabs related to WO_3 that are capped on one side by selenite. The structure of $\text{Ag}_2(\text{MoO}_3)_3\text{SeO}_3$ consists of three crystallographically unique Mo(VI) centers that are also in classical 2 + 2 + 2 coordination environments with two long, two intermediate, and two short bonds. In each MoO_6 unit, three oxygen atoms are shared with four neighboring $[\text{MoO}_6]$ units through edge- and corner-sharing, and with one oxygen atom from the selenite anion. The remaining two oxygen atoms are terminal with O–Mo–O angles of 101.2(2)°, 102.4(2)°, and 102.5(2)° for Mo(1), Mo(2), and Mo(3), respectively. These MoO_6 units are connected to form a molybdenyl ribbon that extends along the *c*-axis as is shown in Fig. 3. Selected bond distances and bond angles are given in Table 5. The BVS

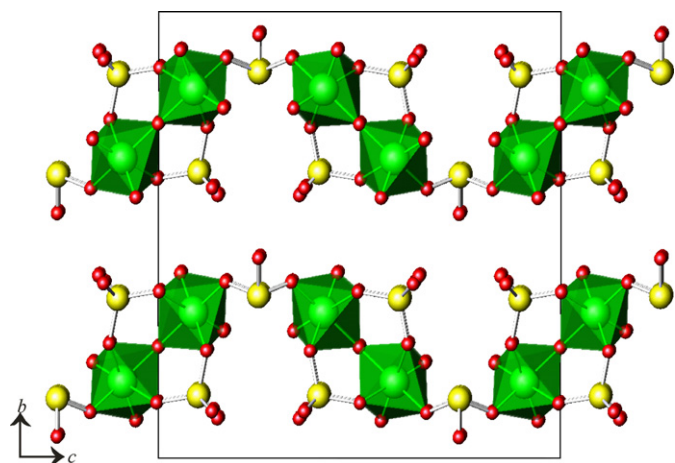


Fig. 1. A view of the one-dimensional $[(\text{Mo}_2\text{O}_5)(\text{SeO}_4)_2(\text{SeO}_3)]^{4-}$ chains that extend down the *c*-axis in the structure of $\text{Ag}_4(\text{Mo}_2\text{O}_5)(\text{SeO}_4)_2(\text{SeO}_3)$.

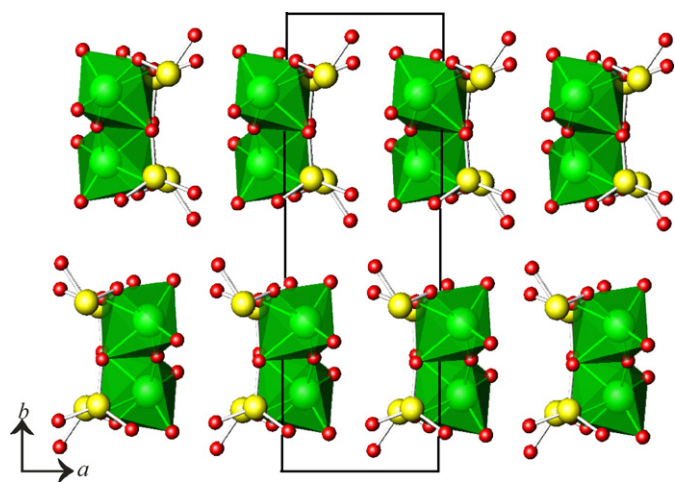


Fig. 2. A depiction of individual polar $[(\text{Mo}_2\text{O}_5)(\text{SeO}_4)_2(\text{SeO}_3)]^{4-}$ chains with the C_2 distortion of the Mo(VI) octahedra aligning on one side of each chain in $\text{Ag}_4(\text{Mo}_2\text{O}_5)(\text{SeO}_4)_2(\text{SeO}_3)$.

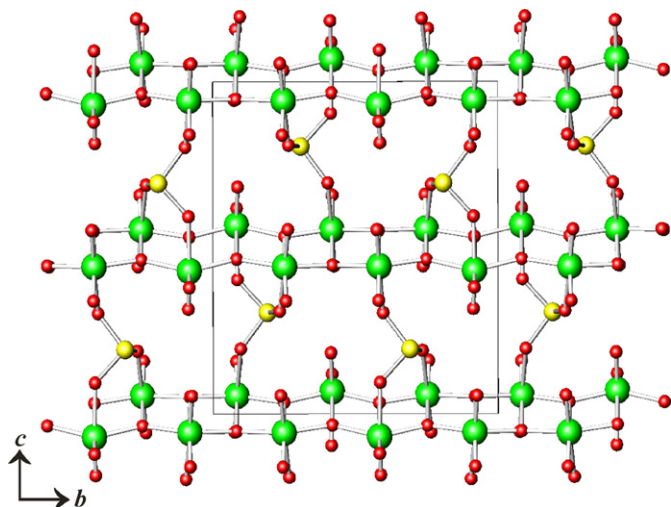


Fig. 3. A view of the two-dimensional $[(\text{MoO}_3)_3\text{SeO}_3]^{2-}$ layer in $\text{Ag}_2(\text{MoO}_3)_3\text{SeO}_3$ that extends in the $[bc]$ plane.

Table 5
Selected bond distances (\AA) and angles (deg) for $\text{Ag}_2(\text{MoO}_3)_3\text{SeO}_3$

Bond distances (\AA)			
Mo(1)–O(1)	1.697(4)	Mo(2)–O(9')	2.373(4)
Mo(1)–O(2)	1.704(3)	Mo(3)–O(4')	1.972(3)
Mo(1)–O(3)	2.300(3)	Mo(3)–O(5)	2.288(4)
Mo(1)–O(4)	1.948(3)	Mo(3)–O(9')	1.951(3)
Mo(1)–O(4')	2.300(4)	Mo(3)–O(10)	1.717(4)
Mo(1)–O(5)	1.942(1)	Mo(3)–O(11)	1.687(4)
Mo(2)–O(5)	1.974(3)	Mo(3)–O(12)	2.236(3)
Mo(2)–O(6)	1.721(4)		
Mo(2)–O(7)	2.152(3)	Se(1)–O(3)	1.711(3)
Mo(2)–O(8)	1.687(4)	Se(1)–O(7)	1.703(3)
Mo(2)–O(9)	1.926(3)	Se(1)–O(12)	1.716(4)
Angles (deg)			
O(1)–Mo(1)–O(2)	101.2(2)	O(7)–Mo(2)–O(9)	82.7(1)
O(1)–Mo(1)–O(3)	82.4(2)	O(7)–Mo(2)–O(9')	79.0(1)
O(1)–Mo(1)–O(4)	103.7(2)	O(8)–Mo(2)–O(9)	104.7(2)
O(1)–Mo(1)–O(4')	166.5(2)	O(8)–Mo(2)–O(9')	169.9(2)
O(1)–Mo(1)–O(5)	106.8(2)	O(9)–Mo(2)–O(9')	74.3(1)
O(2)–Mo(1)–O(3)	176.3(2)	O(4')–Mo(3)–O(5)	72.7(1)
O(2)–Mo(1)–O(4)	98.4(2)	O(4')–Mo(3)–O(9')	107.0(2)
O(2)–Mo(1)–O(4')	92.2(2)	O(4')–Mo(3)–O(10)	95.8(2)
O(2)–Mo(1)–O(5)	96.6(2)	O(4')–Mo(3)–O(11)	102.1(2)
O(3)–Mo(1)–O(4)	81.5(1)	O(4')–Mo(3)–O(12)	83.5(1)
O(3)–Mo(1)–O(4')	84.2(1)	O(5)–Mo(3)–O(9')	75.0(1)
O(3)–Mo(1)–O(5)	176.3(2)	O(5)–Mo(3)–O(10)	96.9(2)
O(4)–Mo(1)–O(4')	72.4(1)	O(5)–Mo(3)–O(11)	160.4(2)
O(4')–Mo(1)–O(5)	73.0(1)	O(5)–Mo(3)–O(12)	77.4(1)
O(5)–Mo(2)–O(6)	91.2(2)	O(9')–Mo(3)–O(10)	94.7(2)
O(5)–Mo(2)–O(7)	82.6(1)	O(9')–Mo(3)–O(11)	106.0(2)
O(5)–Mo(2)–O(8)	106.3(2)	O(9')–Mo(3)–O(12)	83.0(1)
O(5)–Mo(2)–O(9)	145.7(2)	O(10)–Mo(3)–O(11)	102.5(2)
O(5)–Mo(2)–O(9')	72.6(1)	O(10)–Mo(3)–O(12)	174.1(2)
O(6)–Mo(2)–O(7)	166.5(2)	O(11)–Mo(3)–O(12)	83.3(2)
O(6)–Mo(2)–O(8)	102.4(2)		
O(6)–Mo(2)–O(9)	96.1(2)	O(3)–Se(1)–O(7)	98.4(2)
O(6)–Mo(2)–O(9')	87.7(2)	O(3)–Se(1)–O(12)	97.3(2)
O(7)–Mo(2)–O(8)	90.9(2)	O(7)–Se(1)–O(12)	101.5(2)

values of Mo(1), Mo(2), and Mo(3) are 5.99, 6.05, and 5.98, respectively [24,25]. These ribbons are further connected together through tridentate selenite anions to form a two-dimensional layer in $[bc]$ plane, and stacks along a -axis as is shown in Fig. 4. The bridging tridentate selenite anions have Se–O bond distances of 1.703(3), 1.711(3), and 1.716(4) \AA , with a BVS value of 3.94 for the selenium atom [24,25]. Unlike the $A_2(\text{MoO}_3)_3\text{SeO}_3$ ($A = \text{Rb}, \text{Cs}, \text{Tl}, \text{NH}_4$) family of compounds, which have the lone-pair of electrons on the Se atoms located on one side of the molybdenum oxide sheets as indicated by the polar space group, as is shown in Fig. 3, the selenite groups in $\text{Ag}_2(\text{MoO}_3)_3\text{SeO}_3$ have opposing orientations in each layer.

There are two crystallographically unique Ag^+ centers in the structure of $\text{Ag}_2(\text{MoO}_3)_3\text{SeO}_3$. Ag(1) has Ag–O bond distances in the range of 2.400(3)–2.592(3) \AA , while those of Ag(2) range from 2.272(4) to 2.481(3) \AA . Ag(1)O₆ units edge-share with adjacent Ag(2)O₆ polyhedra. The calculated bond valence sums of Ag(1) and Ag(2) are 0.944 and 1.176, respectively [24,25].

3.2.2. Vibrational spectroscopy

The vibrational spectrum of $\text{Ag}_4(\text{Mo}_2\text{O}_5)(\text{SeO}_4)_2(\text{SeO}_3)$ is complex and consist of three primary regions. The highest wavenumber region with three bands observed at 991, 954, and 945 cm^{-1} in IR spectrum and one band at 960 cm^{-1} in Raman spectrum is attributable to vibrational modes from the MoO_2^{2+} units [26]. The second zone has IR bands at 884, 868, 846, 836, and 825 cm^{-1} that can be assigned to stretches of the Se–O bond in the SeO_4^{2-} anions [27]. Finally, two bands in the IR are found at 781 and 726 cm^{-1} that are attributed to the stretches of Se–O bonds in SeO_3^{2-} anions [28]. The Raman spectrum of $\text{Ag}_4(\text{Mo}_2\text{O}_5)(\text{SeO}_4)_2(\text{SeO}_3)$ shows two bands at 815 and 907 cm^{-1} that are due to stretching modes of the SeO_3^{2-} and SeO_4^{2-} , respectively. The IR and Raman spectra of $\text{Ag}_4(\text{Mo}_2\text{O}_5)(\text{SeO}_4)_2(\text{SeO}_3)$ are shown in Fig. 5.

In the IR spectrum of $\text{Ag}_2(\text{MoO}_3)_3\text{SeO}_3$ there are bands at 974, 957, 950, 932, and 911 cm^{-1} that are associated with

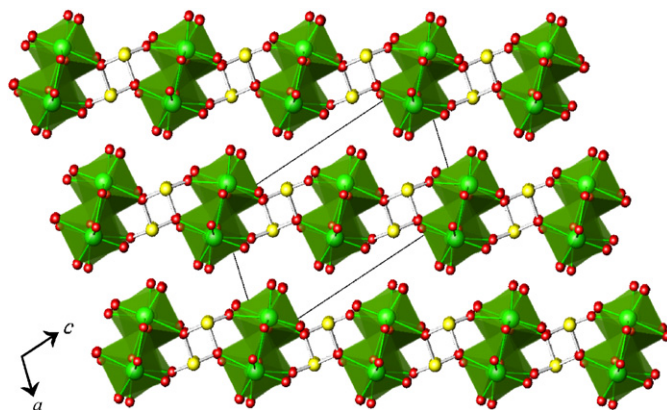
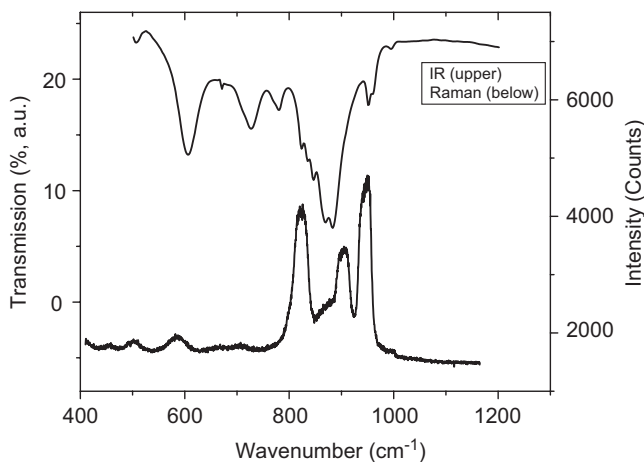
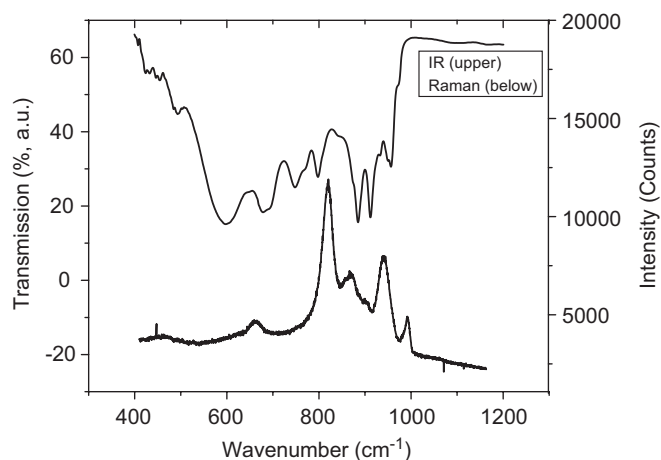


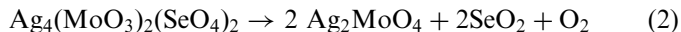
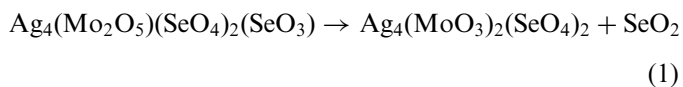
Fig. 4. An illustration of the stacking of the $[(\text{MoO}_3)_3\text{SeO}_3]^{2-}$ layers in $\text{Ag}_2(\text{MoO}_3)_3\text{SeO}_3$.

Fig. 5. IR and Raman spectra of $\text{Ag}_4(\text{Mo}_2\text{O}_5)(\text{SeO}_4)_2(\text{SeO}_3)$.Fig. 6. IR and Raman spectra of $\text{Ag}_2(\text{MoO}_3)_3\text{SeO}_3$.

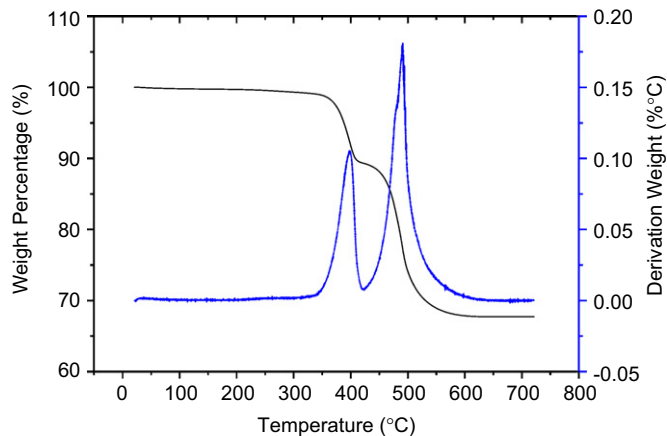
stretches of the molybdenyl units. Five bands at 798, 769, 748, 692, 677, and 599 cm^{-1} are assigned as characteristic vibrational modes for SeO_3^{2-} anions. The Raman spectrum of $\text{Ag}_2(\text{MoO}_3)_3\text{SeO}_3$ shows two sharp bands at 865 and 820 cm^{-1} and one broad band at 664 cm^{-1} that are due to vibrational modes of the SeO_3^{2-} anions. One weak band at 899 cm^{-1} and one sharp band at 942 cm^{-1} are assigned to the stretching modes of the MoO_2^{2+} units. The IR and Raman spectra of $\text{Ag}_2(\text{MoO}_3)_3\text{SeO}_3$ are shown in Fig. 6.

3.2.3. Thermal analysis

The thermal behavior of selenates and selenites is of interest because there are multiple mechanisms of decomposition including loss of oxygen by selenate and decomposition of the selenate and selenite anions to yield SeO_2 [28,29]. The thermal decomposition of $\text{Ag}_4(\text{Mo}_2\text{O}_5)(\text{SeO}_4)_2(\text{SeO}_3)$ follows a two-step mechanism shown in Fig. 7. The TGA curve shows the compound is thermally stable up to 375 °C (Fig. 5). The first step of weight loss is in the temperature range of 376–406 °C, and may correspond to the release of SeO_2 from a SeO_3^{2-} anion. The observed weight loss of 9.95% is in good agreement with the calculated value (9.94%). The second weight loss occurs from 469 to 510 °C can be attributed to the loss of two SeO_2 units and one O_2 molecule released from two SeO_4^{2-} anions. The second experimental weight loss of 22.2% is also consistent with the calculated value (22.7%). The powder X-ray diffraction data of the final residue corresponds with pure Ag_2MoO_4 [30]. Therefore, the two-step decomposition mechanism can potentially be described by the following equations:



Similar to the thermal behavior of $\text{A}_2(\text{MoO}_3)_3\text{SeO}_3$ ($A = \text{Rb}, \text{Cs}, \text{Tl}$) [15], the TGA data for $\text{Ag}_2(\text{MoO}_3)_3\text{SeO}_3$ shows a one-step weight loss over a broad range from 350 to

Fig. 7. A TGA thermogram for $\text{Ag}_4(\text{Mo}_2\text{O}_5)(\text{SeO}_4)_2(\text{SeO}_3)$.

550 °C. The final residue is identified as pure $\text{Ag}_2\text{Mo}_3\text{O}_{10}$ by powder X-ray diffraction [31]. The observed weight loss of 14.1% is close to the theoretical value of 14.3% calculated for the elimination of one SeO_2 from $\text{Ag}_2(\text{MoO}_3)_3\text{SeO}_3$.

4. Conclusions

In this report we have provided the details on the syntheses, structures, vibrational spectroscopy, and thermal behavior of $\text{Ag}_4(\text{Mo}_2\text{O}_5)(\text{SeO}_4)_2(\text{SeO}_3)$ and $\text{Ag}_2(\text{MoO}_3)_3\text{SeO}_3$. Despite the fact that both of these compounds possess oxoanions with a stereochemically active lone-pair of electrons, both compounds crystallize in centrosymmetric space groups. However, both compounds are low-dimensional, a feature that might be attributable to the presence of the selenite anions. Both compounds thermally decompose at elevated temperatures through the loss of SeO_2 .

Acknowledgments

This work was supported by the Chemical Sciences, Geosciences and Biosciences Division, Office of Basic

Energy Sciences, Office of Science, Heavy Elements Program, US Department of Energy under Grant DE-FG02-01ER15187.

References

- [1] H. Effenberger, *Mineral. Petrol.* 36 (1987) 3.
- [2] R.E. Morris, A.P. Wilkinson, A.K. Cheetham, *Inorg. Chem.* 31 (1992) 4774.
- [3] W.T.A. Harrison, Z. Zhang, *Eur. J. Solid State Inorg. Chem.* 34 (1997) 599.
- [4] P.S. Berdonosov, P. Schmidt, O.A. Dityatyev, V.A. Dolgikh, P. Lightfoot, M. Ruck, *Z. Anorg. Allg. Chem.* 630 (2004) 1395.
- [5] I. Krugermann, M.S. Wickleder, *Z. Anorg. Allg. Chem.* 628 (2002) 147.
- [6] J. Baran, T. Lis, M. Marchewka, H. Ratajczak, *J. Mol. Struct.* 250 (1991) 13.
- [7] G. Giester, *Monatsh. Chem.* 120 (1989) 661.
- [8] M. Weil, U. Kolitsch, *Acta Crystallogr. C* 58 (2002) 47.
- [9] G. Giester, *Monatsh. Chem.* 123 (1992) 957.
- [10] M.S. Wickleder, O. Buchner, C. Wickleder, S. el Sheik, G. Brunklaus, H. Eckert, *Inorg. Chem.* 43 (2004) 5860.
- [11] T.A. Sullens, P.M. Almond, J.A. Byrd, J.V. Beitz, T.H. Bray, T.E. Albrecht-Schmitt, *J. Solid State Chem.* 179 (2006) 1192.
- [12] S.V. Krivovichev, I.G. Tananaev, V. Kahlenberg, B.F. Myasoedov, *Dokl. Phys. Chem.* 403 (2005) 124.
- [13] S.V. Krivovichev, I.G. Tananaev, V. Kahlenberg, B.F. Myasoedov, *Radiochemistry* 48 (2006) 217.
- [14] T.E. Albrecht-Schmitt, P.M. Almond, R.E. Sykora, *Inorg. Chem.* 42 (2003) 3788.
- [15] W.T.A. Harrison, L.L. Dussack, A.J. Jacobson, *Inorg. Chem.* 33 (1994) 6043; L.L. Dussack, W.T.A. Harrison, A.J. Jacobson, *Mater. Res. Bull.* 31 (1996) 249.
- [16] P.S. Halasyamani, K.R. Poeppelmeier, *Chem. Mater.* 10 (1998) 2753.
- [17] K.M. Ok, E.O. Chi, P.S. Halasyamani, *Chem. Soc. Rev.* 35 (2006) 710.
- [18] G.M. Sheldrick, *Acta Crystallogr. A* 51 (1995) 33.
- [19] G.M. Sheldrick, SHELXTL PC, Version 5.0, An Integrated System for Solving, Refining, and Displaying Crystal Structures from Diffraction Data, Siemens Analytical X-ray Instrument, Inc., Madison, WI, 1994.
- [20] ATOMS 6.1, Shape Software, 2004.
- [21] N. Kitanovski, A. Golobic, B. Ceh, *Inorg. Chem. Commun.* 9 (2006) 296.
- [22] K.P. Rao, V. Balraj, M.P. Minimol, K. Vidyasagar, *Inorg. Chem.* 43 (2004) 4610.
- [23] D. Xiao, Y. Hou, E. Wang, S. Wang, Y. Li, G. De, L. Xu, C. Hu, *J. Mol. Struct.* 659 (2003) 13.
- [24] I.D. Brown, D. Altermatt, *Acta Crystallogr. B* 41 (1985) 244.
- [25] N.E. Brese, M. O'Keeffe, *Acta Crystallogr. B* 47 (1991) 192.
- [26] E.I. Stiefel, in: G. Wilkinson, R.D. Gillard, J.A. McCleverty (Eds.), *Comprehensive Coordination Chemistry*, vol. 3, Pergamon Press, London, 1978, p. 1380.
- [27] K. Sathjanandan, L.D. McCarty, J.L. Margrave, *Spectrochim. Acta* 20 (1964) 957.
- [28] V.P. Verma, *Thermochim. Acta* 327 (1999) 63.
- [29] D. Havlicek, Z. Micka, R. Boublikova, *Coll. Czech. Chem. Commun.* 60 (1995) 969.
- [30] I. Lindqvist, *Nova Acta Reg. Soc. Sci. Upsa.* 15 (1950) 22.
- [31] B.M. Gatehouse, P. Leverett, *J. Chem. Soc. A* 6 (1968) 1398.